Published in final edited form as:

Curr Biol. 2014 August 4; 24(15): 1689–1699. doi:10.1016/j.cub.2014.06.028.

Tension-Sensitive Actin Assembly Supports Contractility at the Epithelial Zonula Adherens

Joanne M. Leerberg[1], **Guillermo A. Gomez**[1], **Suzie Verma**[1], **Elliott J. Moussa**[1], **Selwin K. Wu**[1], **Rashmi Priya**[1], **Brenton D. Hoffman**[2], **Carsten Grashoff**[3], **Martin A. Schwartz**[4], and **Alpha S. Yap**[1,*]

[1]Division of Molecular Cell Biology, Institute for Molecular Bioscience, The University of Queensland, St. Lucia 4072, Australia

[2]Department of Biomedical Engineering, Duke University, Durham, NC 27708, USA

[3]Group of Molecular Mechanotransduction, Max Planck Institute of Biochemistry, Am Klopferspitz 18, 82152 Martinsried, Germany

[4]Yale Cardiovascular Research Center and Departments of Cardiovascular Medicine, Cell Biology, and Biomedical Engineering, Yale University, New Haven, CT 06520, USA

Summary

Background—Actomyosin-based contractility acts on cadherin junctions to support tissue integrity and morphogenesis. The actomyosin apparatus of the epithelial zonula adherens (ZA) is built by coordinating junctional actin assembly with Myosin II activation. However, the physical interaction between Myosin and actin filaments that is necessary for contractility can induce actin filament turnover, potentially compromising the contractile apparatus itself.

Results—We now identify tension-sensitive actin assembly as one cellular solution to this design paradox. We show that junctional actin assembly is maintained by contractility in established junctions and increases when contractility is stimulated. The underlying mechanism entails the tension-sensitive recruitment of vinculin to the ZA. Vinculin, in turn, directly recruits Mena/VASP proteins to support junctional actin assembly. By combining strategies that uncouple Mena/VASP from vinculin or ectopically target Mena/VASP to junctions, we show that tension-sensitive actin assembly is necessary for junctional integrity and effective contractility at the ZA.

Conclusions—We conclude that tension-sensitive regulation of actin assembly represents a mechanism for epithelial cells to resolve potential design contradictions that are inherent in the

*Correspondence: a.yap@uq.edu.au.

Supplemental Information

Supplemental Information includes Supplemental Experimental Procedures and five figures and can be found with this article online at http://dx.doi.org/10.1016/j.cub.2014.06.028.

Author contributions

J.M.L., G.A.G., and A.S.Y. conceived the project. J.M.L. performed most of the experiments, except for the FRET imaging and western analyses, which were performed by G.A.G. and S.V., respectively. E.J.M. contributed to image analysis. S.K.W. performed the high-resolution characterization of junctional vinculin. R.P. contributed to lentivirus preparation and cell infection. B.D.H., C.G., and M.A.S. developed vinculin FRET sensors and provided assistance and guidance with FRET experiments and manuscript editing. J.M.L., G.A.G., S.V., and E.J.M. quantified the data. J.M.L. and A.S.Y. analyzed the data and wrote the paper.

way that the junctional actomyosin system is assembled. This emphasizes that maintenance and regulation of the actin scaffolds themselves influence how cells generate contractile tension.

Introduction

Cell structure does not always reflect simple design. This is exemplified by the genesis of contractility at the zonula adherens (ZA), a specialized adhesive junction found at the apical-lateral interface in many simple polarized epithelial cells [1, 2]. The ZA is an active mechanical structure where contractile forces are applied to stabilized E-cadherin adhesions [3, 4]. This ultimately generates contractile tension that influences epithelial patterning at the cellular [5, 6] and tissue levels [7].

Consistent with this, the apical ring of E-cadherin that distinguishes the ZA lies contiguous with actomyosin networks that often appear to form prominent perijunctional bundles [8]. This junctional actomyosin unit arises from the dual processes of actin assembly [9, 10] and Myosin activation [4, 8, 11] that are coordinated by E-cadherin adhesions. The actin filaments necessary for the contractile apparatus appear to be assembled at the junctional cortex itself [9], nucleated by Arp2/3, which is recruited to the junction in response to cadherin adhesion [10, 12, 13]. Note that actin assembly is an ongoing feature of established cadherin junctions because steady-state junctional F-actin is reduced when either Arp2/3 or WAVE2 are depleted in epithelial monolayers [10, 13]. Further, this actin assembly apparatus is necessary to support the junctional actomyosin unit because both junctional Myosin II and contractile tension are reduced when Arp2/3 activity is blocked [10].

Contractility at the ZA must ultimately entail the physical interaction of Myosin II and actin filaments. However, this carries a potential design paradox. The branched networks that would be generated when Arp2/3 nucleates actin filaments are commonly thought to be poorly fitted for either the recruitment of Myosin II or the generation of contractile force [14]. Further, Myosin contractility can cause stress-induced F-actin severing [15], leading to turnover of the actin filaments with which it interacts. This represents a challenge that may be especially acute when Myosin interacts with branched actin networks [16]. Such stress-induced F-actin turnover may ultimately limit contractility. Indeed, this occurs at the lateral cadherin junctions found below the ZA, where Myosin II destabilizes Arp2/3-generated actin networks to limit local contractile tension [5]. Nonetheless, junctional F-actin levels remain stable at the ZA, and higher tension is generated there, despite the stresses that may be generated by contractility [5]. Clearly, the cell has strategies to resolve any design incompatibilities that it may encounter at the ZA.

One potential solution to this problem would be for actin assembly at the ZA to increase in response to contractility. This would allow steady-state F-actin content in the junctional cytoskeleton to be preserved despite increased filament turnover. Consistent with this, we found earlier that F-actin content at the ZA of MCF7 cells was significantly reduced by depletion of Myosin II [8]. Analysis of actin dynamics further suggested that Myosin supported a dynamic pool of actin filaments [8]. We have now sought direct evidence for tension-sensitive regulation of actin dynamics at the ZA and endeavored to identify its molecular basis. We focused on vinculin, an actin-regulatory protein that can be found both

at cadherin-based adherens junctions and at integrin-based focal adhesions. The amount of F-actin found at cell-cell junctions is commonly reduced in vinculin-depleted cells [17], but how vinculin regulates the junctional actin cytoskeleton is poorly understood. We now identify vinculin as mediating tension-sensitive actin assembly at the ZA, a process that entails the recruitment of Mena/VASP proteins and is necessary to support junctional contractility itself.

Results

F-Actin Homeostasis at the Zonula Adherens Is Tension-Sensitive

We first analyzed how contractile tension affected F-actin homeostasis at the ZA in confluent Caco-2 monolayers. These polarized colon epithelial cells display prominent zonulae adherentes [2] that are sites of junctional tension [5] and associate with actomyosin bands [4, 5, 9]. Using confocal microscopy to examine the apical plane of the ZA, we assessed steady-state junctional F-actin levels with phalloidin, labeled free barbed ends with Alexa 594-G-actin to identify sites of nucleation and actin assembly, and measured the peak intensity in line scans drawn orthogonal to the junctions to quantitate fluorescence intensity.

As previously reported [9], F-actin concentrates at junctions and in perijunctional cables, whereas free barbed ends are predominantly found at the junctional membrane itself (Figure 1A). Consistent with what we had found earlier in MCF7 cells [8], steady-state F-actin levels were significantly reduced when Caco-2 cells were treated with blebbistatin (50 μM) to block Myosin II (Figures 1A and 1B) or when ROCK was inhibited with Y27632 (data not shown). The implication that actin homeostasis may be Myosin sensitive was confirmed by the demonstration that junctional F-actin levels decreased when either Myosin IIA or Myosin IIB (Figures 1D and S1A available online) were depleted by small hairpin RNA (shRNA) (Figure S1B). Importantly, free barbed-end content at the ZA was also reduced by all these maneuvers that inhibited contractility (Figures 1A, 1C, 1E, and S1A). This implied that contractility supported actin assembly even under steady-state conditions.

We then asked how actin homeostasis responded when contractility at the ZA was increased. To test this, we expressed a Myosin regulatory light-chain transgene (MRLC-DD) bearing phosphomimetic mutations (Thr 18, Ser 19), which can rescue Myosin function when its upstream activators are inhibited [18]. When transiently expressed in Caco-2 cells, MRLC-DD localized to the ZA (Figure S1E) and increased apical junctional tension in those cells (Figures S1C and S1D). Further, junctional F-actin content and barbed-end labeling were increased at the ZA in cells expressing MRLC-DD (Figures 1F, 1G, and S1E). Altogether, this indicated that cells possess a mechanism to tune junctional actin assembly in response to contractile tension.

Vinculin: A Junctional Target for Contractile Tension

In order to identify the molecular basis for tension-sensitive actin assembly, we focused on the actin-binding protein, vinculin, which is found at both integrin- and cadherin-based adhesive junctions [19].Note that vinculin localized specifically to the apical ZA in confluent Caco-2 cells, but not with the E-cadherin clusters found extensively in the lateral

junctions below the ZA (Figure 2A). Thus, vinculin was well placed to influence the actin cytoskeleton at the ZA.

If junctional vinculin were involved in tension-sensitive cellular regulation, we predicted that it might experience molecular-level tension. We tested this using a vinculin transgene bearing a Förster resonance energy transfer (FRET)-based tension sensor (TS) module that reports tensile stretch by a reduction in energy transfer [20]. When expressed in Caco-2 cells, vinculin-TS localized both to the ZA and to focal adhesions (Figure S2A), as does endogenous vinculin. Junctional vinculin-TS generated FRET signals that were conspicuously lower than those from a control vinculin-tailless (TL) mutant, which lacks the F-actin-binding domain of vinculin and is therefore insensitive to tension [20]. This implied that junctional vinculin-TS was under tension at the ZA, as it is in focal adhesions [20]. Consistent with this, Y27632, which reduced contractility at the ZA (data not shown), increased vinculin-TS FRET, signifying reduced molecular tension at the ZA (Figure 2B).

Tension can potentially affect protein function in a number of ways. One possibility is that tension alters the conformation of vinculin itself [21]. Vinculin can exist either in an autoinhibited “closed” conformation, mediated by intramolecular interactions, or in an “open” conformation, where protein-protein interaction motifs are revealed to functionally activate the molecule [19]. To test this notion, we used a conformation-sensitive (CS) biosensor, which incorporates a FRET module within the vinculin backbone (Figures S2B and S2C). This reporter displays high energy transfer when the molecule is in its closed conformation, but it displays decreased energy transfer when the molecule is in its open conformation [22]. When expressed in Caco-2 cells, vinculin-CS displayed greater energy transfer in the cytoplasm than at the ZA (Figures S2B and S2C), consistent with the established concept that cytosolic vinculin exists in the closed, inactive form, whereas that at adhesions is in the open state [20]. However, vinculin-CS FRET at the ZA was not affected by addition of Y27632 (Figure S2C). This implied that the conformation of vinculin at the ZA was not altered by the release of tension, though it may be affected in other contexts [21].

An alternative possibility is that tension regulates the junctional accumulation of vinculin [23, 24]. Indeed, junctional staining of endogenous vinculin was substantially reduced by blebbistatin (Figures 2C and S2D), either Myosin IIA or Myosin IIB shRNA (Figure 2D), or ROCK inhibition (data not shown). Conversely, junctional vinculin was increased when ZA tension was stimulated with MRLC-DD (Figures 2E and S2E). Thus, tension may principally regulate junctional vinculin by controlling its recruitment to the ZA, a notion that is consistent with evidence that its binding partner, α-catenin [25], is tension sensitive [26, 27].

Junctional Vinculin Supports Actin Homeostasis at the ZA

If contractility regulated junctional actin assembly through vinculin, we predicted that depletion of vinculin would affect the junctional cytoskeleton. Indeed, both steady-state F-actin levels (Figures 3A and 3B) and free barbed-end content (Figures 3A and 3C) at the ZA were reduced by vinculin shRNA (Figures S3C and S3E), effects akin to what we had seen when contractility was blocked (Figure 1). These were restored by expression of an RNAi-

resistant vinculin transgene (Figures 5A–5C), confirming that the changes were specific for vinculin.

One caveat, however, was that vinculin at focal adhesions was also reduced by shRNA (Figures S3D and S3F), making it possible that junctional actin homeostasis was indirectly affected by altered focal adhesions. To better define the specific role of junctional vinculin, we used a hybrid molecule (α-catenin-ΔVBS) in which the vinculin-binding domain of α-catenin was replaced by the homologous region of vinculin itself (Figure S3A), thereby ablating the ability of α-catenin to bind vinculin [28]. When expressed in Caco-2 cells depleted of endogenous α-catenin by small interfering RNA (siRNA) (Figure S3C), α-catenin-ΔVBS localized to cadherin junctions (Figure S3B) and reduced junctional vinculin without affecting focal adhesion staining (Figures S3D–S3F). This confirmed that α-catenin-ΔVBS uncouples vinculin recruitment in Caco-2 cells as it does in endothelial cells [28]. Note that both F-actin (Figures 3A and 3B) and barbed-end labeling (Figures 3A and 3C) were reduced at the apical junctions of α-catenin siRNA cells reconstituted with α-catenin-ΔVBS, similar to what we had observed with vinculin shRNA. These findings therefore confirm that the impact of vinculin shRNA on junctional actin homeostasis can be attributed to an action of the junctional vinculin pool.

Finally, we asked whether vinculin depletion affected the response of junctional actin assembly when contractility was stimulated by exogenous MRLC-DD. We found that whereas MRLC-DD increased junctional barbed-end labeling in control cells, this did not occur in vinculin knockdown (KD) cells (Figure 3D). Overall, we conclude that vinculin is necessary for tension-sensitive actin assembly at the ZA.

Vinculin Recruits Ena/VASP Proteins to the ZA

How then might vinculin mediate tension-sensitive actin assembly? Vinculin is a scaffolding protein that can directly bind F-actin and interact with a range of actin-regulatory proteins. These include the Arp2/3 complex [29], which supports actin nucleation at the ZA [10]. This suggested that vinculin might mediate tension-sensitive actin assembly by controlling the recruitment of this nucleator. However, neither junctional Arp3 staining nor localization of WAVE2, the major activator of Arp2/3-mediated nucleation at the ZA in Caco-2 cells [10], were substantively affected by vinculin KD (Figures S4A and S4B). It was therefore unlikely that vinculin simply acted through the Arp2/3-WAVE2 complex.

Ena/VASP proteins are another class of vinculin-binding proteins that can promote actin filament assembly, including assembly at cadherin-based cell-cell junctions [30–33]. Of the three members of this family that are expressed in mammals, we found that both VASP and Mena bound with vinculin in Caco-2 cells and colocalized at the ZA (Figure 4A; Figures S4C and S4E). We were unable to satisfactorily immunostain for Ena-VASP-like protein. Moreover, their junctional localization was impaired in vinculin KD cells and restored by expression of full-length (FL) mouse vinculin (Figures 4A–4C). Because total cellular levels of VASP and Mena were unaffected by vinculin shRNA (Figure S4D), this implied that vinculin might recruit Ena/VASP proteins to the ZA. Consistent with this, we also found that VASP (Figure 4D) and Mena (data not shown) staining at the ZA was reduced when vinculin was selectively uncoupled from junctions by expression of α-catenin-ΔVBS in α-catenin

siRNA cells. Thus, vinculin appeared necessary for VASP and Mena to be recruited to the ZA.

To confirm this, we developed vinculin mutants that specifically uncoupled its ability to bind Ena/VASP proteins. The Ena/VASP binding site in vinculin resides in its polyproline region, which bears a canonical Ena/VASP binding (FPPPP, FP4) motif [34, 35]. We therefore reconstituted vinculin KD cells with vinculin mutants in which either the phenylalanine residue in the FP4 motif was replaced with an alanine (vinculin-AP4) or the complete motif was mutated (Figures S4F–S4H, vinculin-5A). Both these constructs localized to the ZA when expressed in vinculin KD cells (Figure S4G). However, they did not restore the junctional localization of either VASP (Figures 4A and 4B) or Mena (Figure 4C). Therefore, vinculin appears to be a dominant mechanism that recruits Mena/VASP to the ZA.

This further implied that vinculin might support tension-sensitive actin assembly by recruiting Mena/VASP proteins to the ZA. Indeed, we found that junctional VASP (Figures 4E and S4I) and Mena (Figure 4F) were substantially reduced when contractility was inhibited by blebbistatin or by either Myosin IIA or Myosin IIB depletion (Figures 4G and 4H).

Mena/VASP Mediate Regulation of Junctional Actin Homeostasis by Vinculin

We then sought to evaluate what role Mena/VASP proteins played in the tension-sensitive regulation of junctional actin assembly by vinculin. First, we asked whether its ability to bind Mena/VASP was necessary for vinculin to regulate the junctional actin cytoskeleton. We found that whereas expression of FL-vinculin restored both steady-state F-actin levels (Figures 5A and 5B) and barbed-end content (Figures 5A and 5C) to the junctions of vinculin KD cells, these parameters were not restored by expression of either the AP4 or 5A vinculin mutants (Figures 5A–5C). Thus, the ability to bind Mena and VASP appeared crucial for vinculin to regulate junctional actin assembly.

To reinforce the notion that Mena/VASP acted as effectors of vinculin, we asked whether the defective junctional actin assembly seen in vinculin KD cells could be ameliorated if Mena/VASP were restored to junctions. To achieve this, we generated a fusion protein consisting of three tandem FP4 motifs from Listeria ActA fused to the N-terminal domain of α-catenin (Figure S5A, α-Cat-3FP4). The α-catenin fragment in this construct (α-Cat-N) cannot bind F-actin, but it retains its capacity to associate with β-catenin, thereby targeting it to cadherins [36, 37] while the FP4 motifs serve to recruit Ena/VASP. As predicted, α-Cat-3FP4 localized to cell-cell junctions (Figure S5B) and restored junctional Mena and VASP when it was expressed in vinculin KD cells (Figures S5B–S5D). In contrast, α-Cat-N alone localized to junctions but did not recruit Mena or VASP. Therefore, α-Cat-3FP4 could substitute for vinculin to recruit Mena/VASP proteins to junctions.

Expression of α-Cat-3FP4 in vinculin KD cells restored junctional barbed-end content to the same degree as FL-vinculin (Figures 5A and 5C). Therefore, junctional targeting of Mena/VASP could effectively substitute for vinculin in mediating actin assembly. Interestingly, although α-Cat-3FP4 also increased junctional F-actin levels in vinculin KD cells, it did not do so to the same extent as reconstitution of FL-vinculin did (Figure 5B). One possible

reason is because the F-actin networks remained relatively loosely organized at junctions in vinculin KD cells expressing α-Cat-3FP4 (Figure 5A), in contrast to the more condensed F-actin staining seen in control cells or vinculin KD cells expressing FL-vinculin (Figure 5A). This implied that although Mena/VASP are necessary for vinculin to regulate junctional actin filament assembly, vinculin may also influence cytoskeletal organization at junctions by additional mechanisms. Together, these loss-of-function and gain-of-function strategies identified Mena/VASP recruitment as necessary for vinculin to regulate actin assembly at the ZA.

To define the role of Mena/VASP in tension-sensitive actin assembly, we asked how expression of MRLC-DD affected actin assembly when Mena/VASP were not available at the junctions. For this purpose, we expressed a transgene bearing ActA FP4 motifs fused to a mitochondrial targeting sequence (FP4-mito). Earlier, we reported that expression of FP4-mito, but not its inactive mutant, AP4-mito, recruited Ena/VASP proteins to mitochondria and decreased junctional actin assembly [31]. Expression of MRLC-DD increased junctional actin assembly in cells expressing AP4-mito (Figure 5D), as it did in control cells (Figure 1F). However, junctional actin assembly was not increased when MRLC-DD was expressed in FP4-mito cells (Figure 5D). Therefore, Mena/VASP proteins were necessary for contractility to stimulate actin assembly.

Next, we tested whether constitutive targeting of Mena/VASP to junctions might be sufficient to maintain actin assembly even when tension was inhibited. Accordingly, we examined how blebbistatin affected actin assembly when α-Cat-3FP4 was expressed in cells, using a vinculin KD background to eliminate any other potential contributions of vinculin to tension-sensitive actin regulation. Whereas blebbistatin reduced barbed-end labeling in control cells, its impact on junctional actin assembly was substantially blunted in α-Cat-3FP4/Vin KD cells, as shown in Figure 5E. Thus, constitutive targeting of Mena/VASP appeared to render junctional actin assembly resistant to the effects of blebbistatin. This suggested that the vinculin-dependent recruitment of Ena/VASP proteins might be a dominant mechanism for tension to promote actin assembly.

Tension-Sensitive Actin Assembly Supports Contractile Tension and ZA Integrity

Finally, we asked whether tension-sensitive actin assembly was necessary for contractility to be effectively generated at the ZA.

One functional consequence of junctional contractility is ZA integrity itself, which requires the recruitment and activity of both Myosin IIA and Myosin IIB [8]. E-cadherin immunofluorescence revealed that the contiguous apical ring of the ZA was replaced by scattered puncta in vinculin KD cells (Figure 6A), changes akin to what we have observed when Myosin is depleted [8]. Similarly, quantitation of fluorescence intensity confirmed that the accumulation of cadherin at the apical junctions was reduced in vinculin KD cells (Figure 6B). The integrity of the ZA ring was restored to vinculin shRNA cells upon expression of FL-vinculin, confirming the specificity of this effect. However, ZA integrity was not restored by expression of either vinculin AP4 or vinculin 5A, the mutants that uncouple Ena/VASP. This suggested that Mena/VASP-dependent actin assembly was necessary for ZA integrity. This was confirmed by the observation that expression of α-

Cat-3FP4 restored the ZA in vinculin KD cells (Figures 6A and 6B). Total cellular levels of E-cadherin, assessed by immunoblotting cellular lysates (Figure 6C), were unchanged in these cell lines. Therefore, the changes in apical junctional E-cadherin reflected differences in local accumulation at this region rather than altered cellular expression of the cadherin, again consistent with what we have observed when Myosin is inhibited [8].

We then directly examined how junctional tension was influenced by vinculin-dependent actin assembly. Laser nanoscissors were used to cut the apical junctions, and their initial recoil was measured as an index of tension (Figures 6D and 6E). For technical reasons, we monitored the junctions using either E-cadherin-GFP or GFP-tagged vinculin transgenes that localize to the ZA. ZA tension was reduced in vinculin KD cells and restored by FL-vinculin, demonstrating that vinculin supports effective contractility at the ZA (Figure 6D). Tension was not restored if vinculin was uncoupled from Mena/VASP with either the AP4 or 5A mutants (Figure 6E). This implied that maintenance of actin assembly played a key role in allowing vinculin to support junctional tension. Further, tension was restored to vinculin KD cells by expression of α-Cat-3FP4 (Figure 6E). Thus, although the morphology of the apical junction cytoskeleton is not fully restored by the junctional targeting of Mena/VASP, their ability to restore actin assembly is sufficient to support contractile tension at the apical junctions. Together, these findings identify tension-sensitive actin filament homeostasis as part of a feedback mechanism that allows contractility to be maintained at the ZA.

Discussion

Contractility at cadherin junctions generates patterns of tension that influence morphogenetic processes as diverse as apical constriction, cell-on-cell rearrangements, and cell integration into epithelia. However, effective contractility is potentially compromised by the capacity of Myosin II to cause stress-induced actin filament turnover [14–16], thereby limiting the capacity of the actomyosin system to generate force. Indeed, we have recently shown that this occurs at lateral epithelial junctions located below the ZA [5]. Yet, F-actin content and tension are preserved at the apical ZA, implying that cells possess strategies to overcome potential design flaws.

Our current experiments identify tension-sensitive actin assembly as one mechanism at the ZA that allows cells to support junctional contractility. We propose that tension-sensitive recruitment of Mena/VASP proteins allows actin filament assembly at the ZA to be tuned to the level of contractility, thereby compensating for stress-induced filament turnover. This homeostatic pathway exploits the fact that actin assembly is continuously active at the ZA [9, 10, 13, 30], providing an ongoing supply of nascent filaments for the junctional cytoskeleton. Thus, we found that steady-state junctional F-actin content and actin assembly were decreased when the salient elements of the tension-sensitive assembly pathway (vinculin, Mena/VASP) were perturbed. Further, this pathway was also necessary for junctional actin assembly to respond when contractility was stimulated. Functional outcomes of effective contractility, including ZA integrity and junctional tension, required this vinculin-Mena/VASP apparatus to be active. Therefore, tension-sensitive actin assembly is necessary for effective contractility at the ZA.

These findings emphasize the fact that molecular constituents of cadherin junctions can respond to contractile tension. Here, the key is vinculin, which is directly responsible for recruiting Mena/VASP proteins to the ZA and whose junctional localization is tension sensitive. Although other proteins have been reported to recruit Mena/VASP proteins to cadherin junctions [38], vinculin appears to be the predominant mechanism at the ZA in our studies because mutation of its FP4 motif effectively ablated Mena/VASP recruitment to this specialized junction. Alterations in molecular conformation are an important avenue by which vinculin function can be controlled [19]. However, molecular tension across vinculin at the ZA could be reduced by blocking contractility, without any detectable change in its apparent conformation. Instead, the tension-sensitive point in this pathway appears to reside upstream, in the mechanism that recruits vinculin to the ZA. Our results implicate α-catenin in this step because mutation of the vinculinbinding site of α-catenin prevented junctional localization of vinculin. This is consistent with emerging evidence that the capacity of α-catenin to bind vinculin may be regulated by tension [26]. Further, tension sensitivity was lost when Mena/ VASP proteins were constitutively localized at junctions with the α-Cat-3FP4 construct; this reinforces the central role that vinculin plays in making the junctional recruitment of Mena/ VASP respond to tension.

Although vinculin has been known to support the junctional actin cytoskeleton [17], the mechanisms responsible for this were poorly understood. Many processes that affect actin filament dynamics and organization contribute to actin homeostasis at cadherin junctions [39], and vinculin can influence the junctional cytoskeleton in many ways: it can directly bind F-actin, it has the capacity to promote actin assembly in vitro, and it can also bind a wide range of other actin-binding proteins [19]. Our findings argue that vinculin principally regulates actin filament homeostasis at the ZA through Mena/VASP proteins. Thus, Mena/VASP-uncoupled vinculin mutants failed to rescue actin assembly at the ZA in vinculin-depleted cells, but this was restored when Mena/VASP proteins were independently targeted there using the α-Cat-3FP4 fusion protein. Ena/VASP proteins may facilitate actin assembly by protecting barbed ends from premature capping [40] or by functioning as processive actin polymerases [41]. With either mechanism, their action at the ZA underscores the capacity for postnucleation regulators to influence the junctional cytoskeleton.

However, not all of the effects of vinculin can be explained by Mena/VASP because the organization of the junctional actin cytoskeleton was not restored by α-Cat-3FP4. Other mechanisms, such as filament crosslinking [19], may then complement the control of actin dynamics by Mena/VASP to fully account for the impact of vinculin on the ZA cytoskeleton. Vinculin was also recently shown to be tyrosine phosphorylated in response to force at cadherin junctions [42]; whether this affects its ability to regulate the junctional actin cytoskeleton is an interesting open question.

The contribution of Ena/VASP proteins to cell adhesion is best understood in the context of cell migration. In contrast, although members of this protein family can be detected at epithelial cell-cell junctions in a range of tissues and species [30, 31, 43], their role at cell-cell junctions is less clear. Ena/VASP proteins do not appear to be essential for adherens junctions but can promote force-induced strengthening of cadherin adhesions [44]. Our observation that Mena/VASP promote actin filament homeostasis to counteract the effects of

contractility suggests that their contribution to junctional integrity may be most evident when junctions experience stress. Consistent with this, the endothelial barrier that was exposed to shear stress was defective when all Mena/VASP proteins were deleted in mouse embryos [32]. Additionally, in early invertebrate embryos, contributions of Ena are often more evident during dynamic morphogenetic events in which extensive forces are applied to cell-cell junctions [43]. We postulate that loss of tension-sensitive actin assembly may compromise the ability of cells to strengthen adhesion in response to stress.

In conclusion, we propose that tension-sensitive regulation of actin assembly represents a mechanism for epithelial cells to resolve potential design contradictions that are inherent in the way that the junctional actomyosin system is assembled. This emphasizes that maintenance and regulation of the actin scaffolds themselves influence how cells generate contractile tension, in addition to regulation of Myosin II. Although we have focused on the capacity of tension to affect actin filament dynamics, vinculin and Mena/VASP proteins can potentially influence other aspects of actin organization, such as filament bundling, which may also determine the ability of the junctional actin cytoskeleton to support contractility. Moreover, actin assembly via Ena/VASP is not the only mechanism that modulates actin dynamics to support contractility. We recently found that stabilization of actin filaments, mediated by a post-nucleation action of N-WASP [9], is also necessary to allow contractile tension to be generated at the ZA [5]. Thus, distinct molecular mechanisms that mediate different steps in actin filament homeostasis may collaborate to facilitate the contractile apparatus of the ZA. Homologs of Ena/VASP and N-WASP also undergo genetic interactions during C. elegans morphogenesis [45]. It will therefore be interesting to consider whether similar cooperation occurs in other cellular contexts where an effective actomyosin apparatus has to be built.

Experimental Procedures

Cell Culture

Caco-2 cells were maintained in RPMI medium (Gibco) and supplemented with 10% FBS-HI, 1% NEAA, 1% L-glutamine, 100 U/ml penicillin, and 100 U/ml streptomycin.

Immunofluorescence Imaging

Cells were fixed in 4% paraformaldehyde (PFA) in cytoskeletal stabilization buffer (10 mM PIPES [pH 6.8], 100 mM KCl, 300 mM sucrose, 2 mM EGTA, 2 mM $MgCl_2$) on ice for 10 min and subsequently permeabilized with 0.25% Trition X-100 in Tris-buffered saline for 5 min at room temperature. Epi-illumination images were acquired with an IX-81 Olympus microscope (60×objective, 1.4 numerical aperture [NA]) and a Hamamatsu Orca-1 ER camera driven by Metamorph imaging software (version 7; Universal Imaging) or with a Personal DeltaVision inverted widefield deconvolution microscope with a Roper Coolsnap HQ2 camera driven by SoftWoRX software (version 3.7.0). Confocal images were taken using a Zeiss LSM-510 META inverted microscope and a Zeiss LSM-710 FCS inverted microscope driven by ZEN software (ZEN 2009; Zeiss).

G-Actin Incorporation Assay

The incorporation of Alexa 594-labeled G-actin (Invitrogen) into saponin-permeabilized cells has been described previously [12, 46]. Briefly, confluent monolayers of Caco-2 were equilibrated at 25°C for 10 min, then lightly permeablized with 0.2 mg/mL Saponin in permeabilization buffer (138 mM KCl, 4 mM $MgCl_2$; 20 mM HEPES [pH7.4]). Alexa 594-labeled G-actin (0.45 μM; Invitrogen) was added to the cells in permeabilization buffer to favor barbed-end incorporation and was incubated at 25°C for 7 min. The cells were then fixed on ice in 4% PFA in 1×cytoskeletal stabilization buffer containing 0.2% Triton X-100 and Alexa 488 phalloidin for 1 hr.

Quantitation of Fluorescence at Contacts

Quantitative analysis of fluorescence intensity at contacts was performed using the line scan function of ImageJ. A line of 20 μm in length (averaged over 20 pixels) was positioned orthogonal to and centered upon randomly chosen contacts. Numerical values for the fluorescence intensity profile along this line were obtained using the plot profile feature of ImageJ. The baseline of each independent profile was corrected by subtracting a constant value from each of the intensity profiles. A minimum of 50 contacts from three individual experiments were measured. The data from each profile were then imported into Prism 5. Average profiles typically yielded peak-shaped curves, with sides trending to zero, which were then fitted to a Gaussian function. Peak values and their SEs were obtained by nonlinear regression. Statistical analysis was then performed by using two-tailed t test or one-way ANOVA corrected for multiple comparisons, as detailed in the figure legends.

Förster Resonance Energy Transfer

Caco-2 cells were transiently transfected with the vinculin transgene bearing the FRET probe TS, a vinculin-TL biosensor, conformational vinculin sensor (CS), control venus, or teal fluorescent protein constructs. FRET measurements were performed 48 hr after transfection. Cells were imaged live on a LSM 710 Zeiss confocal microscope equipped with a chamber incubator at 37°C. Images were acquired with a 63×objective, 1.4 NA oil Plan Apochromat immersion lens. Donor and FRET channels were recorded by sequential line acquisition using a 458 nm laser line and by collection of the emission in the donor emission region (band pass [BP] 470–500 nm) and acceptor emission region (BP 530–560 nm), respectively. In addition, crosstalk and acceptor images were acquired by using the 514 nm laser line for excitation and by collecting the emission in the donor and acceptor emission regions. For FRET measurements, raw images were filtered to correct for photonic noise using a median filter of 1 pixel radius [47]. The corrected FRET (cFRET) signal for images from the FRET channel was calculated pixel by pixel using the following equation [20]:

$$\mathrm{cFRET}=\mathrm{FRET}-\mathrm{Dbt}(\mathrm{I_D})\times\mathrm{DONOR}-\mathrm{Abt}(\mathrm{I_A})\times\mathrm{ACEPTOR}$$

Where FRET is the FRET channel images, $Dbt(I_D)$ and $Abt(I_A)$ are the donor and acceptor bleed-through functions expressed as functions of donor (I_D) and acceptor (I_A) intensities, and DONOR and ACEPTOR are the donor and acceptor images, respectively.

$Dbt(I_D)$ and $Abt(I_A)$ functions and cFRET calculations were performed as described previously [20], using a custom-written MATLAB routine. The FRET index was calculated for every image as the average (FRET/Acceptor) emission ratio for pixels located in the selected regions of interest (ROIs) drawn on raw images, and the data presented correspond to pooled data from three independent experiments.

Laser Nanoscissors

Nanoscissors experiments were performed on a LSM 510 META Zeiss confocal microscope equipped with a 37°C heating stage. Images were acquired with a 63× objective, 1.4 NA oil Plan Apochromat immersion lens at 2× digital magnification. A total of six frames were acquired with an interval of 8 s per frame. The Ti Sapphire laser (Chameleon Ultra, Coherent Scientific) was tuned to 790 nm for the ablation of cell-cell contacts labeled with either E-cad-TdTomato or GFP. A constant ROI (3.8 × 0.6 μm) was positioned with the longer axis perpendicular to the cell-cell contact. Contacts were ablated with 30 iterations of 790 nm laser at 24% transmission.

Using MTrackJ plugin (ImageJ), the distance (d) between vertices that define the ablated contact was measured as a function of time (t). Distance values after ablation were subtracted from the initial contact length, d(0). The values of d(t) − d(0) were averaged across a minimum of 30 contacts from three independent experiments, and, subsequently, the initial recoil values and their SEs were obtained by nonlinear regression of the data to the following equation:

$$f(t)=\frac{\text{Initial recoil}}{k}(1-e^{-kt})$$

Finally, statistical analysis for initial recoil values between different groups was performed by ANOVA or t test, as described in the corresponding figure legends.

Detailed experimental procedures related to siRNA knockdown, plasmids and shRNA reagents, antibodies, and immunoprecipitation are included in the Supplemental Experimental Procedures.

Supplementary Material

Refer to Web version on PubMed Central for supplementary material.

Acknowledgments

We thank our laboratory colleagues for their unceasing support and fellowship, and we thank our many colleagues who generously provided reagents for this project. This work was supported by funding from the NHMRC Australia (1010489, 1037320, 1044041), the Australian Research Council (DP120104667), and the Kids' Cancer Project of the Oncology Children's Foundation. J.M.L. was supported by an Australian Postgraduate Award, S.K.W. was supported by a University of Queensland Research Scholarship, and R.P. was supported by an ANZ Trustees PhD Scholarship in Medical Research. A.S.Y. is a Research Fellow of the NHMRC. Optical microscopy was performed at the ACRF/IMB Cancer Biology Imaging Facility, established with the generous support of the ACRF. C.G. is supported by the German Research Council (GR3399-2.1) and the Max Planck Society. B.D.H. is supported by the Searle Scholars Program and by a Basil O'Connor Starter Scholar Award from the March of Dimes. M.A.S. was supported by NIH PO1 GM98412.

References

1. Farquhar MG, Palade GE. Junctional complexes in various epithelia. J. Cell Biol. 1963; 17:375–412. [PubMed: 13944428]
2. Meng W, Mushika Y, Ichii T, Takeichi M. Anchorage of microtubule minus ends to adherens junctions regulates epithelial cell-cell contacts. Cell. 2008; 135:948–959. [PubMed: 19041755]
3. Priya R, Yap AS, Gomez GA. E-cadherin supports steady-state Rho signaling at the epithelial zonula adherens. Differentiation. 2013; 86:133–140. [PubMed: 23643492]
4. Ratheesh A, Gomez GA, Priya R, Verma S, Kovacs EM, Jiang K, Brown NH, Akhmanova A, Stehbens SJ, Yap AS. Centralspindlin and α-catenin regulate Rho signalling at the epithelial zonula adherens. Nat. Cell Biol. 2012; 14:818–828. [PubMed: 22750944]
5. Wu SK, Gomez GA, Michael M, Verma S, Cox HL, Lefevre JG, Parton RG, Hamilton NA, Neufeld Z, Yap AS. Cortical F-actin stabilization generates apical-lateral patterns of junctional contractility that integrate cells into epithelia. Nat. Cell Biol. 2014; 16:167–178. [PubMed: 24413434]
6. Blankenship JT, Backovic ST, Sanny JS, Weitz O, Zallen JA. Multicellular rosette formation links planar cell polarity to tissue morphogenesis. Dev. Cell. 2006; 11:459–470. [PubMed: 17011486]
7. Martin AC, Gelbart M, Fernandez-Gonzalez R, Kaschube M, Wieschaus EF. Integration of contractile forces during tissue invagination. J. Cell Biol. 2010; 188:735–749. [PubMed: 20194639]
8. Smutny M, Cox HL, Leerberg JM, Kovacs EM, Conti MA, Ferguson C, Hamilton NA, Parton RG, Adelstein RS, Yap AS. Myosin II isoforms identify distinct functional modules that support integrity of the epithelial zonula adherens. Nat. Cell Biol. 2010; 12:696–702. [PubMed: 20543839]
9. Kovacs EM, Verma S, Ali RG, Ratheesh A, Hamilton NA, Akhmanova A, Yap AS. N-WASP regulates the epithelial junctional actin cytoskeleton through a non-canonical post-nucleation pathway. Nat. Cell Biol. 2011; 13:934–943. [PubMed: 21785420]
10. Verma S, Han SP, Michael M, Gomez GA, Yang Z, Teasdale RD, Ratheesh A, Kovacs EM, Ali RG, Yap AS. A WAVE2-Arp2/3 actin nucleator apparatus supports junctional tension at the epithelial zonula adherens. Mol. Biol. Cell. 2012; 23:4601–4610. [PubMed: 23051739]
11. Shewan AM, Maddugoda M, Kraemer A, Stehbens SJ, Verma S, Kovacs EM, Yap AS. Myosin 2 is a key Rho kinase target necessary for the local concentration of E-cadherin at cell-cell contacts. Mol. Biol. Cell. 2005; 16:4531–4542. [PubMed: 16030252]
12. Kovacs EM, Goodwin M, Ali RG, Paterson AD, Yap AS. Cadherin-directed actin assembly: E-cadherin physically associates with the Arp2/3 complex to direct actin assembly in nascent adhesive contacts. Curr. Biol. 2002; 12:379–382. [PubMed: 11882288]
13. Tang VW, Brieher WM. α-Actinin-4/FSGS1 is required for Arp2/3-dependent actin assembly at the adherens junction. J. Cell Biol. 2012; 196:115–130. [PubMed: 22232703]
14. Yang Q, Zhang XF, Pollard TD, Forscher P. Arp2/3 complex-dependent actin networks constrain myosin II function in driving retrograde actin flow. J. Cell Biol. 2012; 197:939–956. [PubMed: 22711700]
15. Medeiros NA, Burnette DT, Forscher P. Myosin II functions in actin-bundle turnover in neuronal growth cones. Nat. Cell Biol. 2006; 8:215–226. [PubMed: 16501565]
16. Reymann AC, Boujemaa-Paterski R, Martiel JL, Guérin C, Cao W, Chin HF, De La Cruz EM, Théry M, Blanchoin L. Actin network architecture can determine myosin motor activity. Science. 2012; 336:1310–1314. [PubMed: 22679097]
17. Taguchi K, Ishiuchi T, Takeichi M. Mechanosensitive EPLIN-dependent remodeling of adherens junctions regulates epithelial reshaping. J. Cell Biol. 2011; 194:643–656. [PubMed: 21844208]
18. Jordan P, Karess R. Myosin light chain-activating phosphorylation sites are required for oogenesis in Drosophila. J. Cell Biol. 1997; 139:1805–1819. [PubMed: 9412474]
19. Carisey A, Ballestrem C. Vinculin, an adapter protein in control of cell adhesion signalling. Eur. J. Cell Biol. 2011; 90:157–163. [PubMed: 20655620]
20. Grashoff C, Hoffman BD, Brenner MD, Zhou R, Parsons M, Yang MT, McLean MA, Sligar SG, Chen CS, Ha T, Schwartz MA. Measuring mechanical tension across vinculin reveals regulation of focal adhesion dynamics. Nature. 2010; 466:263–266. [PubMed: 20613844]

21. Dumbauld DW, Lee TT, Singh A, Scrimgeour J, Gersbach CA, Zamir EA, Fu J, Chen CS, Curtis JE, Craig SW, García AJ. How vinculin regulates force transmission. Proc. Natl. Acad. Sci. USA. 2013; 110:9788–9793. [PubMed: 23716647]
22. Chen H, Choudhury DM, Craig SW. Coincidence of actin filaments and talin is required to activate vinculin. J. Biol. Chem. 2006; 281:40389–40398. [PubMed: 17074767]
23. Peng X, Cuff LE, Lawton CD, DeMali KA. Vinculin regulates cell-surface E-cadherin expression by binding to beta-catenin. J. Cell Sci. 2010; 123:567–577. [PubMed: 20086044]
24. Miyake Y, Inoue N, Nishimura K, Kinoshita N, Hosoya H, Yonemura S. Actomyosin tension is required for correct recruitment of adherens junction components and zonula occludens formation. Exp. Cell Res. 2006; 312:1637–1650. [PubMed: 16519885]
25. Choi HJ, Pokutta S, Cadwell GW, Bobkov AA, Bankston LA, Liddington RC, Weis WI. αE-catenin is an autoinhibited molecule that coactivates vinculin. Proc. Natl. Acad. Sci. USA. 2012; 109:8576–8581. [PubMed: 22586082]
26. Yonemura S, Wada Y, Watanabe T, Nagafuchi A, Shibata M. alpha-Catenin as a tension transducer that induces adherens junction development. Nat. Cell Biol. 2010; 12:533–542. [PubMed: 20453849]
27. Barry AK, Tabdili H, Muhamed I, Wu J, Shashikanth N, Gomez GA, Yap AS, Gottardi CJ, de Rooij J, Wang N, Leckband DE. α-catenin cytomechanics—role in cadherin-dependent adhesion and mechanotransduction. J. Cell Sci. 2014; 127:1779–1791. [PubMed: 24522187]
28. Huveneers S, Oldenburg J, Spanjaard E, van der Krogt G, Grigoriev I, Akhmanova A, Rehmann H, de Rooij J. Vinculin associates with endothelial VE-cadherin junctions to control force-dependent remodeling. J. Cell Biol. 2012; 196:641–652. [PubMed: 22391038]
29. DeMali KA, Barlow CA, Burridge K. Recruitment of the Arp2/3 complex to vinculin: coupling membrane protrusion to matrix adhesion. J. Cell Biol. 2002; 159:881–891. [PubMed: 12473693]
30. Vasioukhin V, Bauer C, Yin M, Fuchs E. Directed actin polymerization is the driving force for epithelial cell-cell adhesion. Cell. 2000; 100:209–219. [PubMed: 10660044]
31. Scott JA, Shewan AM, den Elzen NR, Loureiro JJ, Gertler FB, Yap AS. Ena/VASP proteins can regulate distinct modes of actin organization at cadherin-adhesive contacts. Mol. Biol. Cell. 2006; 17:1085–1095. [PubMed: 16371509]
32. Furman C, Sieminski AL, Kwiatkowski AV, Rubinson DA, Vasile E, Bronson RT, Fässler R, Gertler FB. Ena/VASP is required for endothelial barrier function in vivo. J. Cell Biol. 2007; 179:761–775. [PubMed: 17998398]
33. Baum B, Perrimon N. Spatial control of the actin cytoskeleton in Drosophila epithelial cells. Nat. Cell Biol. 2001; 3:883–890. [PubMed: 11584269]
34. Brindle NP, Holt MR, Davies JE, Price CJ, Critchley DR. The focal-adhesion vasodilator-stimulated phosphoprotein (VASP) binds to the proline-rich domain in vinculin. Biochem. J. 1996; 318:753–757. [PubMed: 8836115]
35. Reinhard M, Rüdiger M, Jockusch BM, Walter U. VASP interaction with vinculin: a recurring theme of interactions with proline-rich motifs. FEBS Lett. 1996; 399:103–107. [PubMed: 8980130]
36. Watabe-Uchida M, Uchida N, Imamura Y, Nagafuchi A, Fujimoto K, Uemura T, Vermeulen S, van Roy F, Adamson ED, Takeichi M. alpha-Catenin-vinculin interaction functions to organize the apical junctional complex in epithelial cells. J. Cell Biol. 1998; 142:847–857. [PubMed: 9700171]
37. Maddugoda MP, Crampton MS, Shewan AM, Yap AS. Myosin VI and vinculin cooperate during the morphogenesis of cadherin cell cell contacts in mammalian epithelial cells. J. Cell Biol. 2007; 178:529–540. [PubMed: 17664339]
38. Hansen MD, Beckerle MC. Opposing roles of zyxin/LPP ACTA repeats and the LIM domain region in cell-cell adhesion. J. Biol. Chem. 2006; 281:16178–16188. [PubMed: 16613855]
39. Brieher WM, Yap AS. Cadherin junctions and their cytoskeleton(s). Curr. Opin. Cell Biol. 2013; 25:39–46. [PubMed: 23127608]
40. Bear JE, Gertler FB. Ena/VASP: towards resolving a pointed controversy at the barbed end. J. Cell Sci. 2009; 122:1947–1953. [PubMed: 19494122]
41. Hansen SD, Mullins RD. VASP is a processive actin polymerase that requires monomeric actin for barbed end association. J. Cell Biol. 2010; 191:571–584. [PubMed: 21041447]

42. Bays JL, Peng X, Tolbert CE, Guilluy C, Angell AE, Pan Y, Superfine R, Burridge K, DeMali KA. Vinculin phosphorylation differentially regulates mechanotransduction at cell-cell and cell-matrix adhesions. J. Cell Biol. 2014; 205:251–263. [PubMed: 24751539]

43. Gates J, Mahaffey JP, Rogers SL, Emerson M, Rogers EM, Sottile SL, Van Vactor D, Gertler FB, Peifer M. Enabled plays key roles in embryonic epithelial morphogenesis in Drosophila. Development. 2007; 134:2027–2039. [PubMed: 17507404]

44. Kris AS, Kamm RD, Sieminski AL. VASP involvement in force-mediated adherens junction strengthening. Biochem. Biophys. Res. Commun. 2008; 375:134–138. [PubMed: 18680720]

45. Sheffield M, Loveless T, Hardin J, Pettitt J. Celegans Enabled exhibits novel interactions with N-WASP, Abl, and cell-cell junctions. Curr. Biol. 2007; 17:1791–1796. [PubMed: 17935994]

46. Verma S, Shewan AM, Scott JA, Helwani FM, den Elzen NR, Miki H, Takenawa T, Yap AS. Arp2/3 activity is necessary for efficient formation of E-cadherin adhesive contacts. J. Biol. Chem. 2004; 279:34062–34070. [PubMed: 15159390]

47. Stepensky D. FRETcalc plugin for calculation of FRET in non-continuous intracellular compartments. Biochem. Biophys. Res. Commun. 2007; 359:752–758. [PubMed: 17555710]

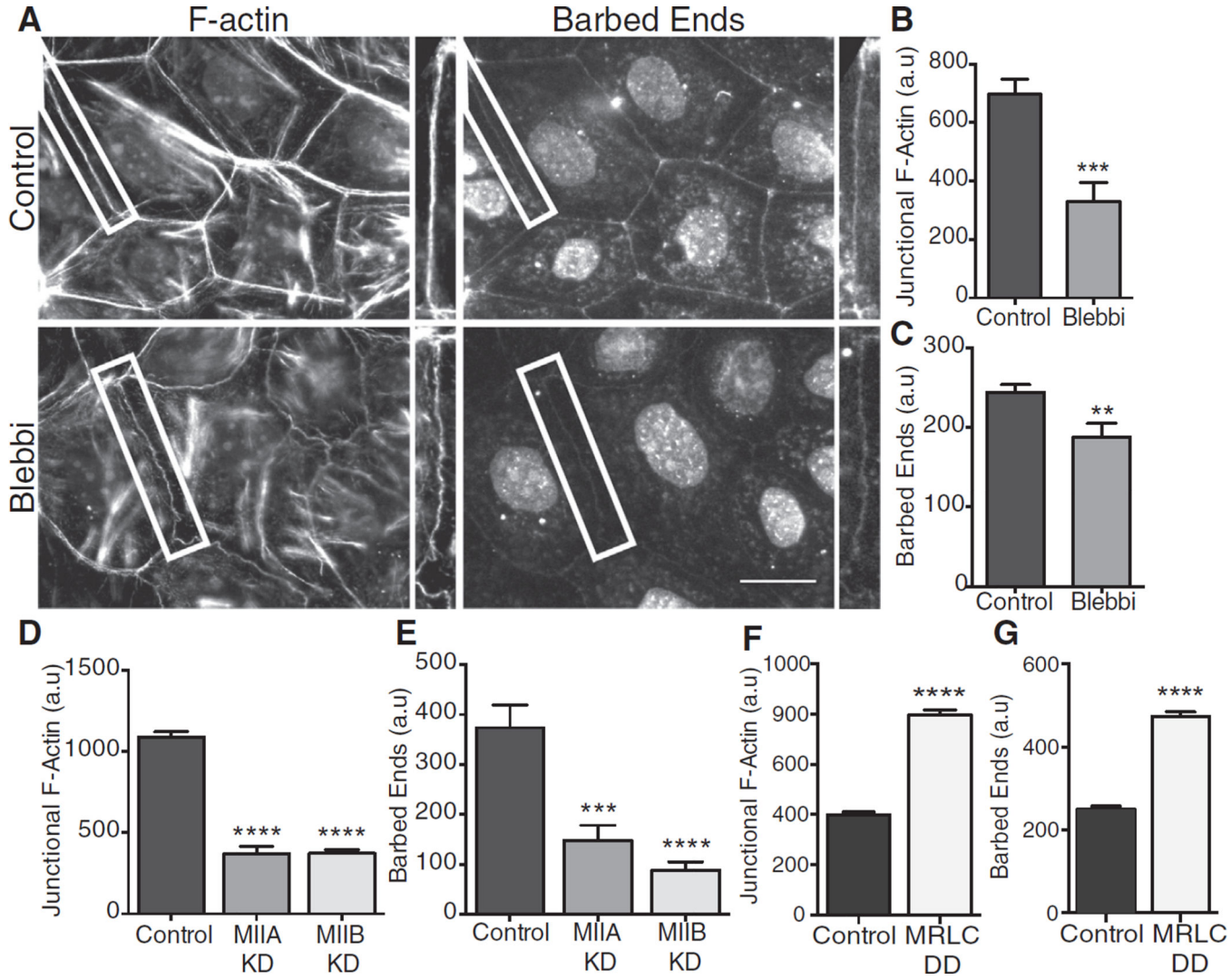

Figure 1. F-Actin Homeostasis at the Epithelial Zonula Adherens Is Tension Sensitive

(A) Representative images of F-actin (phalloidin) and barbed-end labeling (G-actin incorporation) at the apical junctions of control and blebbistatin-treated (Blebbi) Caco-2 cell monolayers. Rectangles mark detailed junctional regions shown on the right side of each panel. Scale bar represents 20 μm.

(B and C) Quantitation of apical junction F-actin (B) and barbed-end labeling (C) upon treatment with blebbistatin (50 μM).

(D and E) Apical junctional F-actin (D) and barbed-end labeling (E) in Myosin IIA (MIIA KD) or Myosin IIB (MIIB KD) shRNA cells.

(F and G) Apical junctional F-actin (F) and barbedend labeling (G) in cells expressing MRLC-DD. Data show mean ± SEM (n = 3 biological replicates). **p < 0.01, ***p < 0.001, ****p < 0.0001, compared with controls; one-way ANOVA, Tukey's multiple comparisons test.

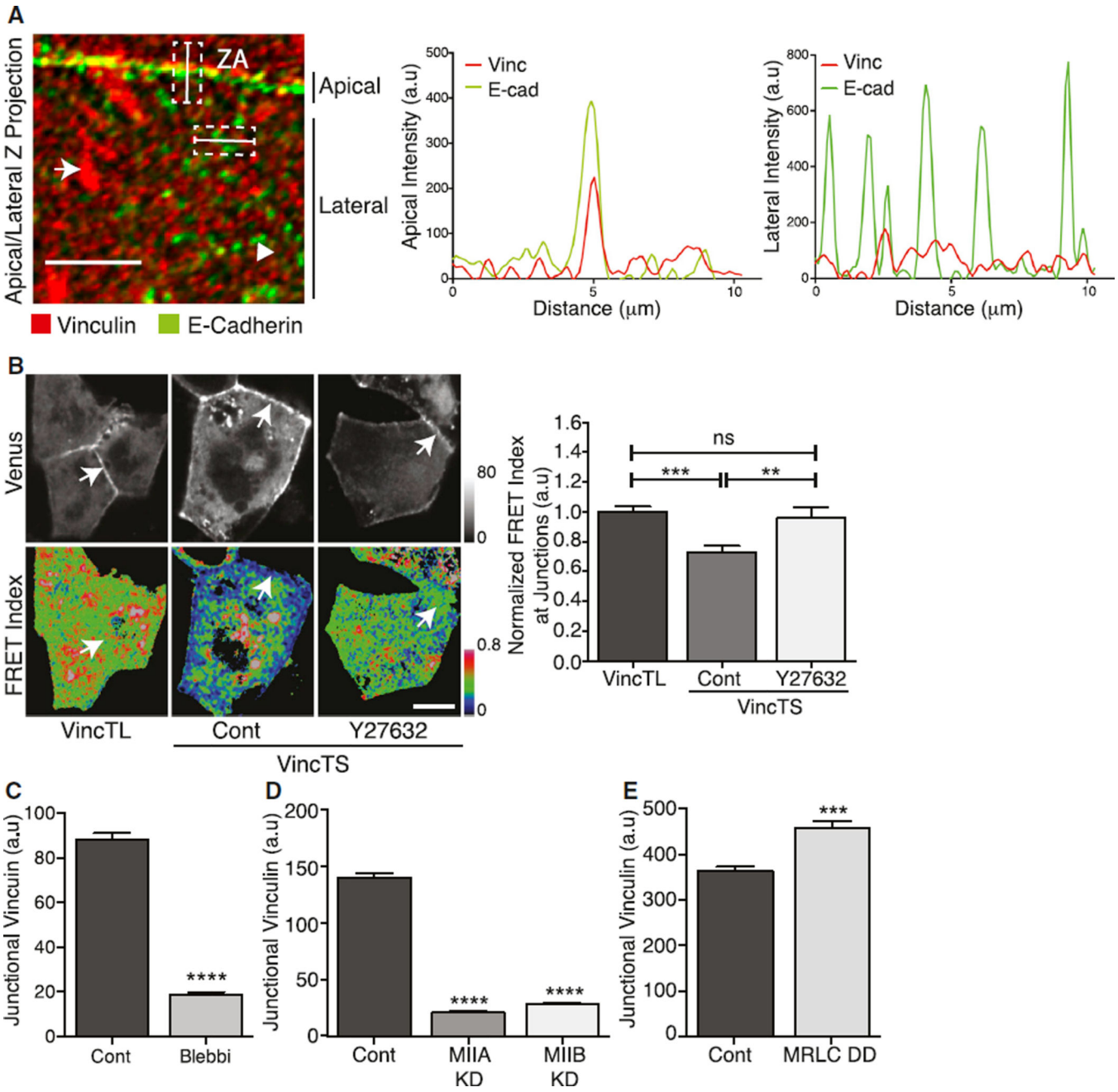

Figure 2. Vinculin Is a Target for Contractile Tension at the Zonula Adherens

(A) Localization of vinculin and E-cadherin within cell-cell junctions. Maximum projection view of E-cadherin (green) and vinculin (red) immunostaining at an en face (slanted) cell-cell junction is shown. ZA position is indicated. Arrow indicates focal adhesion (vinculin); triangle indicates lateral cluster (E-cadherin). Line scan analysis of the indicated lines (white) confirms that vinculin colocalizes with E-cadherin at the ZA, but not with E-cadherin clusters in the lateral junctions. Scale bar represents 5 μm.

(B) Molecular tension across vinculin at the ZA. FRET index images (left) and quantitation (right) for vinculin-TS or for a control vinculin construct lacking the actin-binding domain

(TL) in the presence or absence of Y27632 are shown. Scale bar represents 20 μm. Data show mean ± SEM for at least 60 images per condition, pooled from four independent experiments. One-way ANOVA, Sidak's multiple comparison test.

(C–E) Junctional vinculin at the ZA when contractility was inhibited with blebbistatin (C) or Myosin II shRNA (D) or when contractility was stimulated by expression of MRLC-DD (E). Data show mean ± SEM (n = 3 biological replicates). ns, not significant; **p < 0.01, ***p < 0.001, ****p < 0.0001, compared with controls; one-way ANOVA, Tukey's multiple comparisons test.

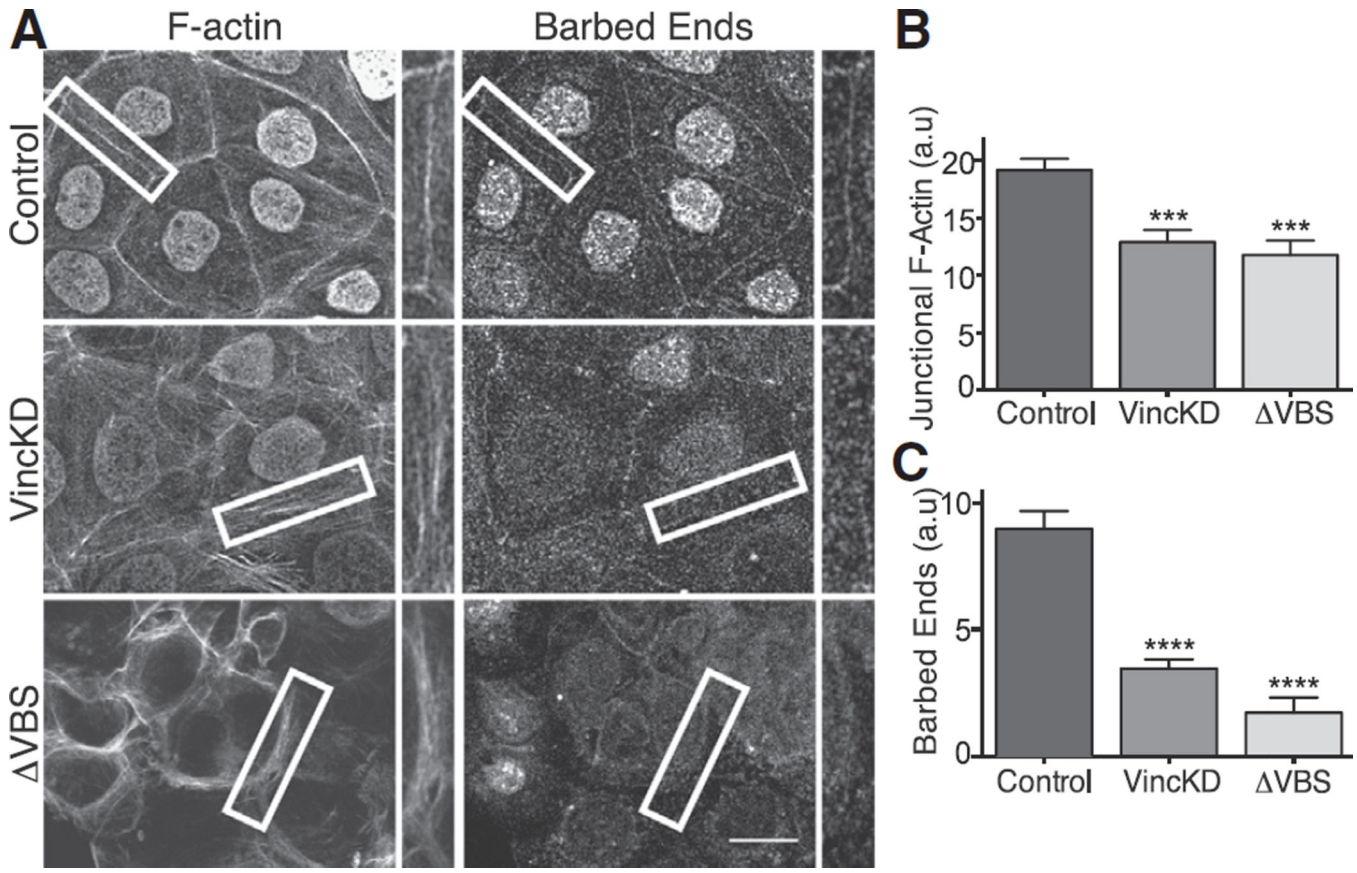

Figure 3. Junctional Vinculin Regulates Actin Filament Assembly at the Zonula Adherens

(A) Representative confocal images (and details, marked in boxes) of F-actin and barbed-end labeling at the apical junctions in control cells, vinculin shRNAcells, and α-catenin siRNAcells expressing α-catenin ΔVBS. Note that nuclear fluorescence reflects nuclear localization signal-GFP infection marker. Scale bar represents 20 μm.

(B and C) Quantitation of junctional F-actin (B) and barbed-end labeling (C) in the conditions mentioned in (A).

(D) Quantitation of barbed-end labeling in control and vinculin shRNA cells, with or without MRLC-DD expression.

Data show mean ± SEM (n = 3 biological replicates). ns, not significant; ***$p < 0.001$, ****$p < 0.0001$, compared as indicated; one-way ANOVA, Tukey's multiple comparisons test.

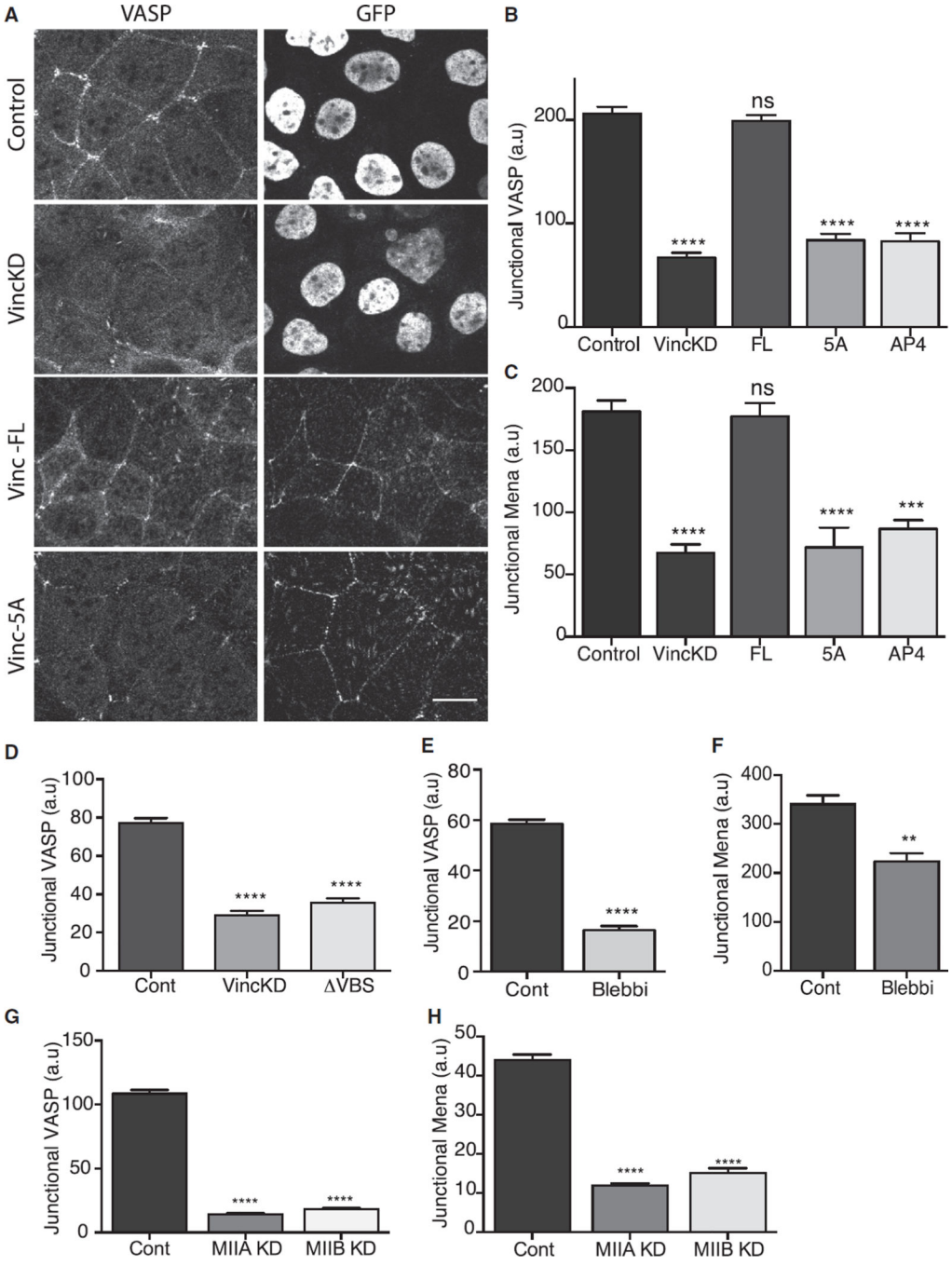

Figure 4. Mena/VASP Are Recruited to the ZA by Vinculin in a Tension-Sensitive Manner

(A) Effect of vinculin shRNA (KD) on junctional localization of VASP and its restoration by FL-vinculin and vinculin transgenes mutant for the FP4 motif. GFP was used to identify infected cells: control and vinculin shRNA viruses encoded GFP bearing a nuclear-localization signal, whereas the vinculin transgenes were tagged with GFP. Scale bar represents 20 μm.

(B and C) Quantitation of junctional VASP (B) and Mena (C) in vinculin shRNA cells reconstituted with FL and mutant vinculin.

(D) Junctional VASP in control cells, vinculin shRNA cells, and α-catenin siRNA cells expressing α-catenin ΔVBS.
(E and F) Effect of blebbistatin on junctional VASP (E) or Mena (F).
(G and H) Effect of Myosin IIA shRNA or Myosin IIB shRNA on junctional VASP (G) or junctional Mena (H).
Data show mean ± SEM (n = 3 biological replicates). ns, not significant; **p < 0.01, ***p < 0.001, ****p < 0.0001, compared with controls; one-way ANOVA, Tukey's multiple comparisons test.

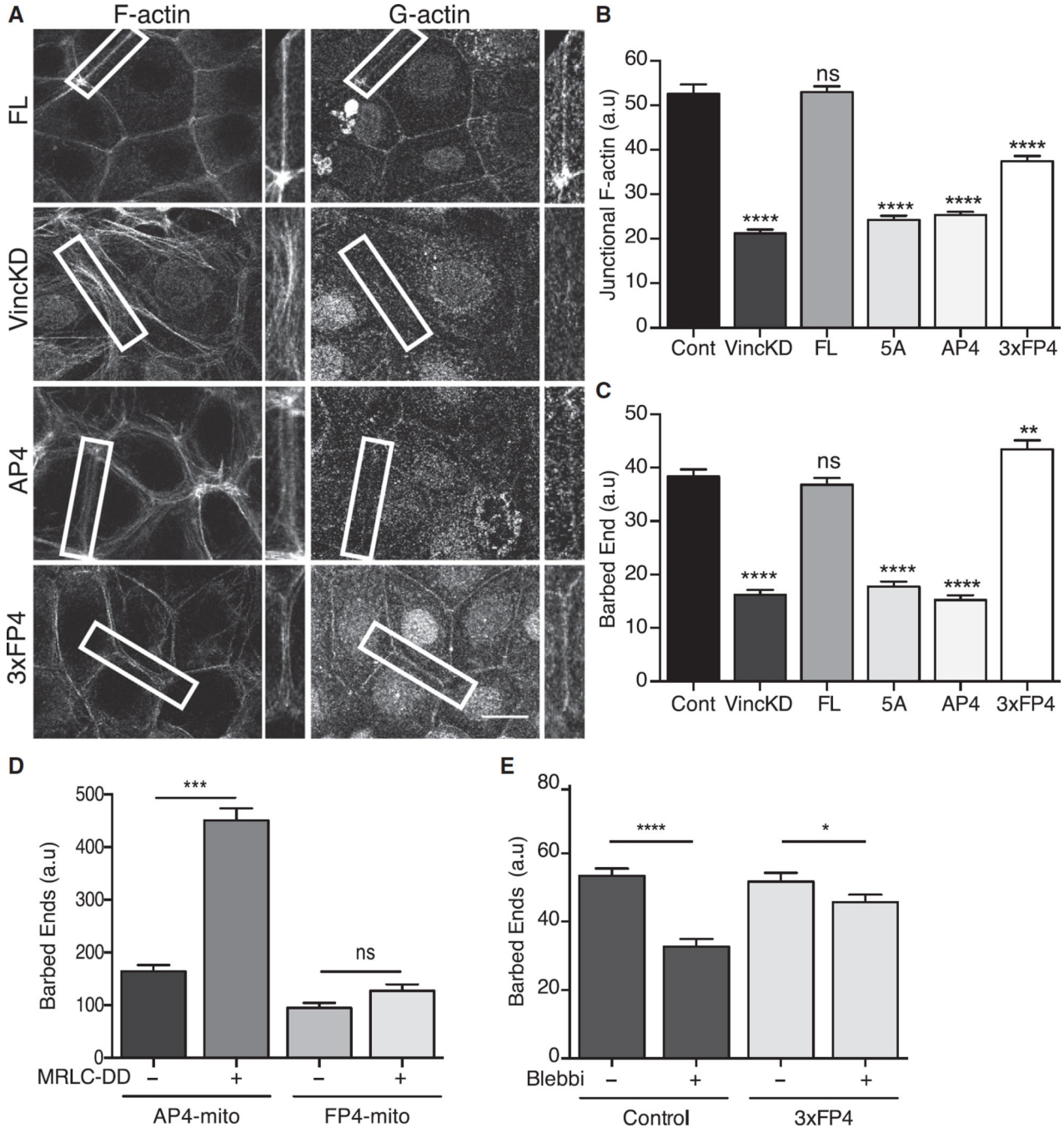

Figure 5. Junctional Mena/VASP Are Necessary Effectors of Tension-Sensitive Actin Assembly

(A–C) Interaction with Mena/VASP proteins is necessary for vinculin to support junctional actin assembly. F-actin and barbed-end labeling at the ZA were examined in vinculin KD cells and KD cells reconstituted with FL-vinculin, vinculin transgenes mutated in the Mena/VASP-binding site (AP4, 5A), or a cadherin-targeted Mena/VASP-binding fusion protein (3xFP4). Representative images are shown in (A), with quantitation of junctional F-actin (B) and barbed-end labeling (C). Scale bar of (A) represents 20 μm.

(D) Mena/VASP proteins are necessary for contractility to stimulate junctional actin assembly. GFP-MRLC-DD or GFP (control) were coexpressed with AP4-mito or FP4-mito, and barbed-end labeling was measured at the apical junctions.

(E) Effect of blebbistatin on junctional actin assembly in control cells or vinculin KD cells expressing α-Cat-3FP4 (3xFP4).

Data show mean ± SEM (n = 3 biological replicates), except for (D), where data show mean ± SD (n = 2 biological replicates). ns, not significant; *p < 0.5, ** p < 0.01, ***p < 0.001, ****p < 0.0001, compared with controls or as indicated; one-way ANOVA, Tukey's multiple comparisons test.

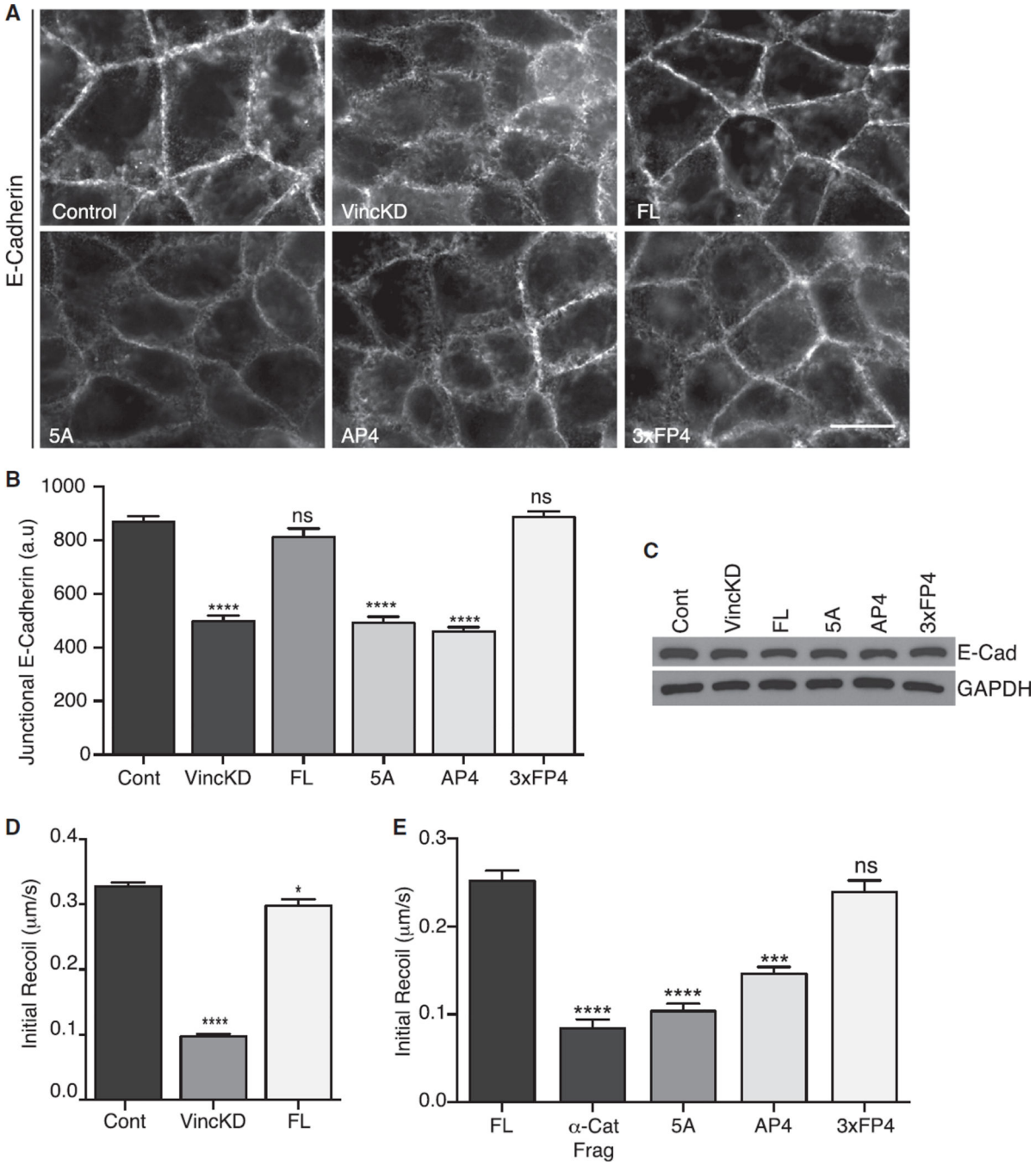

Figure 6. Tension-Sensitive Actin Assembly Is Necessary for ZA Integrity and Junctional Tension

ZA integrity and junctional tension in control cells (Cont), vinculin shRNA cells (VincKD), and vinculin KD cells reconstituted with a FL-vinculin transgene, vinculin transgenes bearing mutations in the Mena/VASP-binding site (5A, AP4), or α-Cat-3FP4 (3xFP4). (A and B) Representative images of E-cadherin staining at the apical planes (A) and quantitation of apical junctional cadherin accumulation (B). Scale bar of (A) represents 20 μm.

(C) Western blot analysis of total cellular levels of E-cadherin. GAPDH was used as a loading control.

(D and E) The effect of vinculin KD on junctional tension at the ZA measured by laser nanoscissors (D) and the role for Mena/VASP recruitment to junctions (E).

Data show mean ± SEM of 30 contacts, pooled from three biological replicates. ns, not significant; *$p < 0.05$, ***$p < 0.001$, ****$p < 0.0001$, compared with controls; nonlinear regression, one-phase association and one-way ANOVA, Tukey's multiple comparisons test.